Analysis of MRI Data Monitoring the Treatment of Polycystic Kidney Disease in a Preclinical Mouse Model

S. Hadjidemetriou[1], W. Reichardt[1], J. Hennig[1], M. Buechert[2], and D. von Elverfeldt[1]
[1]Department of Diagnostic Radiology, University Hospital Freiburg, Freiburg, Germany, [2]MRDAC, Freiburg, Germany

Introduction: Autosomal dominant polycystic kidney disease (ADPKD) is characterized by the growth of cysts in the kidneys that increase their volume, disrupt their normal function, and lead to kidney failure in humans [1,2]. A clinically approved treatment for this condition is not yet available. An essential step for the development of medical treatments is preclinical treatment studies with an in-vivo mouse model of the condition [2]. In this study treated as well as untreated mice have been monitored longitudinally with a high field MRI animal scanner. The manual analysis of such data is labor intensive, subjective, and not exactly reproducible. This work presents a reliable method for the unsupervised segmentation of mouse kidneys. The foreground and the kidney region of interest in an image is first identified and restored for imaging artifacts. That region is analyzed for its statistics and used to estimate geometric models for the kidneys. They provide seeds and serve as priors for the graph cut segmentation algorithm that delineates the kidney contours. The performance of the algorithm has been validated extensively.

Image acquisition: Three groups each of four genotype mice models of ADPKD were used [2]. The first group was treated with rapamycin, the second with vasopressin-2-receptor antagonist SR121463, and the control group was untreated. The mice were imaged with a 9.4Tesla MRI animal scanner at six representative time points that gave a total of 6×12=72 images. The mice were anesthetized and cardiac gating was used. The acquisition sequences were a T2w RARE and a T1w FLASH. For both sequences the field of view was coronal of 30×30mm^2 and a matrix of size 256×256. Thus, the in-plane voxel resolution is 0.12×0.12mm^2. The slice thickness was 0.50mm without slice spacing. On average twenty-five slices were included to ensure a complete coverage of both kidneys. Example slices are shown in Figure 1(a-b). The T1w image was co-registered rigidly to the higher contrast T2w image with Mattes mutual information [3].

Image analysis: The noise in the image background is modeled with a Rayleigh distribution. The largest connected component in the remaining signal region provides the foreground occupied by tissues. The mean point and first eigenvector over the binarized tissue regions provide the mid-sagittal axis. The point between the two kidneys is identified as the one along the axis with maximum Gaussian filter response. The mean points of the kidneys are initialized around it and are varied to maximize the sum of intensities in a super-spheroid centered at these points and with major axes parallel to the mid-sagittal axis. The optimization is performed with gradient descent. The union of the spherical regions surrounding the mean kidney points is the region of interest (ROI). The ROI is restored for intensity uniformity [4].

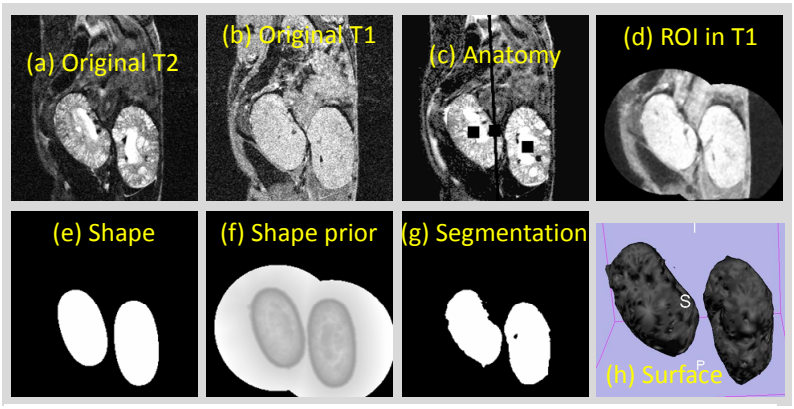

Figure 1. Processing of a mid-sagittal slice.

A kidney is approximated in its side of the ROI with a parameterized geometric super-spheroid. The registration of the shape is for translation, coronal rotation, uniform scaling, and eccentricity. The registration maximizes the mutual information with gradient descent. The intensity auto-co-occurrence statistics of the T1w and the T2w images are analyzed separately in the ROI using Otsu's algorithm to identify the distributions that correspond exclusively to the foreground, exclusively to the background, and an intermediate range of ambiguity. The registered shape together with the back-projections of the intensity statistics to the image determine the foreground and background seeds. They initialize the graph cut segmentation algorithm that resolves the ambiguous voxels lying out of the seeds to provide the kidney contours [5]. The neighborhood weights of the graph consider both the intensities of the T2w image and of the co-registered T1w image. The spatio-intensity distance from the contours of the registered super-spheroids is computed and serves as a shape prior by modulating the neighborhood weights of the graph. The weights also consider voxel anisotropy. The processing steps for an example slice are shown in Figure 1(c-g) and a rendering of the kidneys' surfaces is shown in Figure 1(h). The implementation is in C++ and uses the ITK library [3].

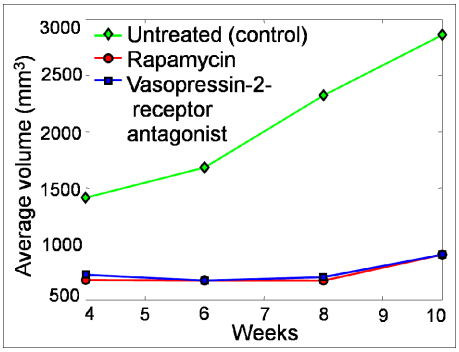

Figure 2 Longitudinal volumetric analysis.

Results and discussion: The automated analysis was compared with manual kidney contour annotations C_M performed by a medical expert for all 72 images. The volumes of the true positive, V_{TP}, false negative, V_{FN}, and false positive, V_{FP}, provide a volume based comparison in terms of the recall, RE=$V_{TP}/(V_{TP}+V_{FN})$, and precision, PR=$V_{TP}/(V_{TP}+V_{FP})$. Their average and standard deviation over all the images were RE=93.10±3.96% and PR=94.10±3.70%. The automatically localized contour, C_A, and C_M have also been compared. The infimum distance maps from C_A to C_M averaged over C_M, $\langle d_{A\to M}\rangle_M$, and vice versa, $\langle d_{M\to A}\rangle_A$, were computed independently and averaged to provide the symmetric mean absolute surface distance d_{AM}. Its average and standard deviation over all the images was d_{AM}=3.28±1.91pixels or d_{AM}=0.64±0.37mm. The validation demonstrates the high accuracy of the analysis. The surrogate marker of disease progression is the average within group kidney volume [1,2]. It is plotted in Figure 2 and shows that both treatments have succeeded in halting the increase in kidney volume and thus the progression of the condition. This is consistent with the results obtained with previous more invasive and interactive methods [1,2]. The analysis methods presented can accelerate the rate of preclinical treatment trials for ADPKD.

References:

[1] Walz, G., Nephrol. Dial Transplant., 21(7), (2006)
[2] Reichardt, W., Romaker, D., Becker, A., Buechert, M., Walz, G., Elverfeldt, D., MAGMA, 22(3), (2008)
[3] Ibanez, L., Schroeder, W., Ng, L., Cates, J.: The ITK Software Guide. Kitware, Inc. ISBN 1-930934-15-7, 2nd Edition, (2005)
[4] Hadjidemetriou, S., Studholme, C., Mueller, S., Weiner, M., Schuff, N., Medical Image Analysis 13 (1), (2009)
[5] Boykov, Y., Lea, G.: Graph cuts and efficient N-D image segmentation. IJCV, 70(2), (2006)